

# A Melamine-Based Polyimide as Filler in P84 Mixed Matrix Membrane for Increasing Permeability in O<sub>2</sub>/N<sub>2</sub> Separation

Xiaoxu Yuan<sup>1,2</sup>, Quanping Wu<sup>1\*</sup>, Yue Zhang<sup>2</sup>, Guoxiong Deng<sup>2</sup>, Yilei Wang<sup>2\*</sup>, Xueping Zong<sup>2</sup>, Song Xue<sup>2</sup>

<sup>1</sup>Tianjin Key Laboratory of the Design and Intelligent Control of the Advanced Mechanical System, School of Mechanical Engineering, Tianjin University of Technology, Tianjin, 300384, China; <sup>2</sup>Tianjin Key Laboratory of Organic Solar Cells and Photochemical Conversion, School of Chemistry and Chemical Engineering, Tianjin University of Technology, Tianjin, 300384, China

## ABSTRACT

A Mixed Matrix Membrane (MMM) was developed for improving O<sub>2</sub>/N<sub>2</sub> selectivity by using a polyimide covalent organic framework (PI-COF) as filler. The PI-COF powder was synthesized by heating melamine and 3,3',4,4'-biphenyl tetracarboxylic dianhydride (BPDA) at 200°C through solvothermal reaction. The structure of PI-COF was characterized by FT-IR, SEM, and XRD. Commercial P84 polyimide membrane blended with the PI-COF afforded a larger permeability of N<sub>2</sub> than that of O<sub>2</sub>. At 0.1 MPa, N<sub>2</sub> and O<sub>2</sub> had the permeability of 466 and 219 barrer, respectively, and the ideal gas selectivity of 2.13 was achieved at the loading 20% PI-COF. Through this mixed matrix membrane prepared from simple synthesis and low cost of the starting materials, it provided an alternative polyimide COF as filler to oxygen-enriched air for commercial uses.

**Keywords:** Covalent organic framework; Mixed matrix membrane; Polyimide; Air separation; Permeability

## INTRODUCTION

In the high energy-consumption industries, such as metallurgy, polycrystalline silicon, and petroleum refining, we have no choice but to elevate energy efficiency because of a global oil shortage. Enriched oxygen instead of air is an effective way of reducing energy consumption in the fuel combustion system [1]. Only pumping excess air into the combustion system could not solve the problem as the heat energy would be wasted by taking away through the increased exhaust gas flow. For the utilization of pure oxygen, the cost for preparation and storage become a severe economic burden. When the oxygen is enriched in the range of 25-30 wt%, the quantity of NO<sub>x</sub> in the emission after fuel burning could be cut down significantly and the burning strength, speed up the burning rate, increase the flame temperature and heat utilization could also be enhanced [2-4]. In a natural gas furnace at the temperature of 1648°C, around 32% of natural gas could be saved when the oxygen concentration in the air reached 30% [5]. Therefore, the low-grade fuel could be used in the kilns and furnaces instead of high-quality one using the oxygen-enriched air.

For example, the lignite coal with enriched oxygen (26.7 wt%) have the same flame temperature with the heavy oil burning in ordinary air. Therefore, it is much attractive to find an economical way to prepare the oxygen-enriched air for fuel combustion.

To achieve the oxygen-enriched air, the membrane enrichment process shows the advantages of the low requirement to the equipment, easy operation, and unrestricted scale-up, compared to traditional pressure swing adsorption and deep cooling process. Membranes for oxygen enrichment have been actively investigated and both inorganic and organic materials have been applied to get better enrichment performance [6,7]. As inorganic membranes are high cost and harsh to process and install, the organic membranes are widely accepted by the industry [8]. The greatest challenge for gas membrane enrichment is the compromise between permeability and selectivity. As Robson mentioned in his work, among the polymeric membranes, Mixed Matrix Membrane (MMM) had the highest upper bound in the plot of log permeability versus log selectivity, which was located closest to the commercial application area [9]. To further enhance the both selectivity and permeability

**Correspondence to:** Quanping Wu, Tianjin Key Laboratory of the Design and Intelligent Control of the Advanced Mechanical System, School of Mechanical Engineering, Tianjin University of Technology, Tianjin, 300384, China, Fax: +86-22-60214252; E-mail: wqping@ustc.edu.cn  
Yilei Wang, Tianjin Key Laboratory of Organic Solar Cells and Photochemical Conversion, School of Chemistry and Chemical Engineering, Tianjin University of Technology, Tianjin, 300384, China, Fax: +86-22-60214252; E-mail: wang0549@e.ntu.edu.sg

**Received:** May 05, 2019; **Accepted:** May 16, 2019; **Published:** May 22, 2019

**Citation:** Yuan X, Wu Q, Zhang Y, Deng G, Wang Y, Zong X, et al. (2019) A Melamine-Based Polyimide as Filler in P84 Mixed Matrix Membrane for Increasing Permeability in O<sub>2</sub>/N<sub>2</sub> Separation. *J Membr Sci Technol* 9: 196. doi: 10.4172/2155-9589.1000196

**Copyright:** © 2019 Yuan X, et al. This is an open-access article distributed under the terms of the Creative Commons Attribution License, which permits unrestricted use, distribution, and reproduction in any medium, provided the original author and source are credited.

in gas separation, various types of fillers, such as porous zeolites [10], carbon nanotubes [11], carbon sieve [12] and halloysite nanotubes [13], have been incorporated into the polymer matrix to disorder the molecule chain arrangement and finally increase the gas permeability.

Recently, the Covalent Organic Frameworks (COF) with controllable porous structure and tunable organic groups become the potential candidates for MMM preparation [14-17]. The covalent bonds between monomers in the framework gave COFs higher thermal and chemical stability [16,18]. Due to their uniform porous structure and adjustable functional groups, these COFs attracted attention in gas membrane enrichment. In Gascon's group, the selectivity for CO<sub>2</sub>/N<sub>2</sub> could reach 35 using an azine-linked COF as filler in a Matrimid-based MMM, while the permeability is 17.7 barrer [15]. The permeability of 14.8 barrer was also reported using TpBD/polybenzimidazole membrane [19]. The COF-based polymeric membranes showed excellent selectivity but low permeability. For O<sub>2</sub>/N<sub>2</sub> separation, it is still a big challenge due to their similar molecular dynamic diameter (0.346 nm/0.364 nm) [20-25]. Most polymeric membranes provided the O<sub>2</sub>/N<sub>2</sub> separation efficiency in the range of 0.9-10 [26-31]. Before enrichment, the feeding air should be pre-compressed because it needs the energy to go through the membrane. If the membrane prefers interception of nitrogen molecules, the oxygen-enriched air is on the permeate side with low pressure. So, the energy is wasted as the oxygen molecules pass through the membrane. Conversely, if N<sub>2</sub> permeates the membrane faster than O<sub>2</sub>, the oxygen-enriched air could be collected on the feeding side with a certain pressure. The energy for compressing air is saved and the pressured oxygen-enriched air could be directly fed into the combustion system. At this point, developing a nitrogen prior penetration membrane has a great application potential.

In this work, a PI-COF mixed P84 membrane was prepared for O<sub>2</sub>/N<sub>2</sub> separation oxygen enrichment. The PI-COF was used as filler due to its correct pore structure and easy synthesis. Melamine was chosen as a cheap triamine for the preparation PI-COF by reaction with biphenyltetracarboxylic Dianhydride (BPDA). The COF morphology, thermal stability, and chemical structure were characterized by field emission Scanning Electron Microscope (SEM), Thermal Gravimetric Analysis (TGA), and Fourier Transport Infrared Spectrometer (FT-IR). The pure gas permeability of nitrogen and oxygen was respectively tested by the permeation measurement equipment. The PI-COF supports us a possible way to prepare oxygen-enriched air through nitrogen prior penetration.

## EXPERIMENTAL

### Materials

Melamine was purchased from Tianjin Guangfu Fine Chemical Research Institute (China). 3,3',4,4'-Biphenyl Tetracarboxylic Dianhydride (BPDA) was obtained from China Tech (Tianjin) Chemical Co., Ltd. Anhydrous methanol, acetone, Dimethylacetamide (DMAC) and Dimethyl Sulfoxide (DMSO) was commercially available from Tianjin Benchmark Chemical Reagent Co., Ltd. P84 (BTDA-TDI/MDI, copolyimide of 3,3',4,4'-benzophenone tetracarboxylic dianhydride, 80 wt% methylphenylene-diamine and 20 wt% methylene diamine) was purchased from HP Polymer GmbH, Austria. The polymer was dried overnight at 80°C under vacuum before use. The as-synthesized PI-COF particles were activated under vacuum at 100°C for 12 h before use.

### Synthesis of PI-COF

The powders of melamine (1 g) and BPDA (5.8 g) were mixed together before dropping into the poly (tetrafluoroethylene) inner tank of the solvothermal reactor which contained 5 mL DMAC inside. Then the reactor was stored in an oven for 20 h at 200°C. The PI-COF was collected after washing three times with DMSO. The collected brownish-yellow powder was sonicated in the methanol for 1 h. Then the powders were immersed into acetone for another 12 h. After repeating this step for three times, the PI-COF was dried in a vacuum oven and milled for characterization and membrane preparation.

### Membrane preparation

For membrane preparation, certain amounts of PI-COF particles were added into a 20 wt% solution of P84 in DMAc. All the casting solutions were stirred at room temperature overnight to form a uniform solution. The solution was then cast onto the clean glass slides with a 50 μm casting knife at a moving speed of 2.5 cm/s. The casting solution coated slides were moved into a vacuum oven at 80°C and dried for 24 h. The ratio ( of PI-COF in MMMs were 10%, 20%, 30% and 40 wt% in this study (based on equation 1).

$$r = \frac{m_{COF}}{m_{P84}} \times 100\% \quad (1)$$

Where  $m_{COF}$  and  $m_{P84}$  are the mass of PI-COF and P84 in the MMMs, respectively.

### Characterization

The X-ray diffraction (XRD) was collected from a Rigaku Ultima IVX-ray Diffractometer (40 kV and 40 mA) with Cu Kα ( $\lambda=0.15406$  nm) radiation at a scanning rate of 2°C/min from 2°C to 60°C. The morphology of samples was taken with a Zeiss merlin Compact scanning electron microscope at 5.0 kV. The samples were attached onto conductive double-sided carbon adhesive and coated with platinum before observation. FTIR measurements were carried out using a Perkin Elmer 782 Fourier transform spectrophotometer. Thermo gravimetric analysis (TGA) was performed with a TA instruments Q500 at a heating rate of 10°C min<sup>-1</sup> under nitrogen. The BET surface and pore size distribution of imide-linked COF was measured via a Quantachrome NOVA4000 after degassing at 573 K for 3 hours. BET surface area was calculated over the range of relative linear portion of the BET plot. Pore size distribution was calculated from the adsorption and desorption branch of the N<sub>2</sub> adsorption isotherm using the Barrett-Joyner-Halenda (BJH) formula.

### Gas permeation tests

Pure gas transport properties of the P84 membrane and the PI-COF doped membranes were measured in the order of N<sub>2</sub> and O<sub>2</sub> at 302.15 K and 0.1 MPa using the constant-pressure and variable-volume method. The air in the frame cell was exhausted by feeding gas for 10 min. While the system was at a steady state, nitrogen or oxygen was flowed across the flat membrane surface in the frame cell, which had an effective area of 3.0 cm<sup>2</sup>. The feeding pressure was controlled by a backpressure valve and the permeate stream were directly introduced into a soap bubble flow meter. Permeability ( $P$ , barrer) was calculated as equation (2) below, according to the average value of five tests:

$$P = \frac{l}{A \cdot \Delta p} \times \frac{273.15}{T} \times \frac{p_0}{76} \times \left( \frac{dV}{dt} \right) \quad (2)$$

Where  $A$  is the effective membrane area,  $p$  is the cross membrane pressure,  $T$  is the temperature,  $p_0$  is the atmospheric pressure,  $l$  is the thickness of MMM to be tested and  $dV/dt$  is the volumetric displacement rate.

The ideal selectivity for two gases is determined as equation (3):

$$\alpha = \frac{P_{N_2}}{P_{O_2}} \quad (3)$$

Where  $P_{N_2}$  and  $P_{O_2}$  are the permeability of pure  $N_2$  and  $O_2$ , respectively.

## RESULTS AND DISCUSSION

### Characterization of PI-COF

PI-COF was synthesized by heating melamine and BPDA in a solvothermal reactor at 200°C for 20 h (Figure 1a). The powders were washed with DMSO. After filtration, the brownish-yellow PI-COF was washed with methanol with sonication and then was immersed in acetone to remove the residual solvent as clear as possible. Notably, both melamine and BPDA are planar molecules and finally were polymerized into a porous crystalline structure. As shown in Figure 1b, the powder XRD patterns of the as-synthesized PI-COF have intense diffraction peaks, confirming the existence of well crystallinity. The  $\langle 001 \rangle$  diffraction peak at 27.2° corresponds to an interlayer distance of  $\sim 3.4$  Å, suggesting a typical van der Waals contact between the aromatic layers of the PI-COF. To the contrary, the amorphous P84 particles have broad peaks in the XRD pattern indicating its amorphous structure. The FT-IR spectrum of PI-COF shows absorptions at 1535  $\text{cm}^{-1}$  and 1469  $\text{cm}^{-1}$ , indicating the quadrant and semicircle stretching of the triazine ring (Figure 2). The  $\text{O}=\text{C}-\text{O}-\text{C}=\text{O}$  vibration at 1855 and 1784  $\text{cm}^{-1}$  for the starting compound BPDA decreased considerably, and the strong absorptions at 1768 and 1734  $\text{cm}^{-1}$  can be attributed to the newly formed  $\text{O}=\text{C}-\text{N}-\text{C}=\text{O}$  group of imide ring, assigning to asymmetric and symmetric

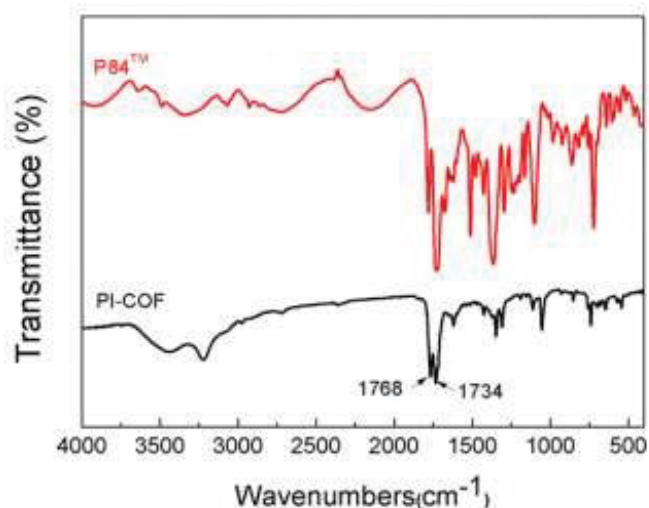


Figure 2: FT-IR spectra of PI-COF (black) and P84 (red).

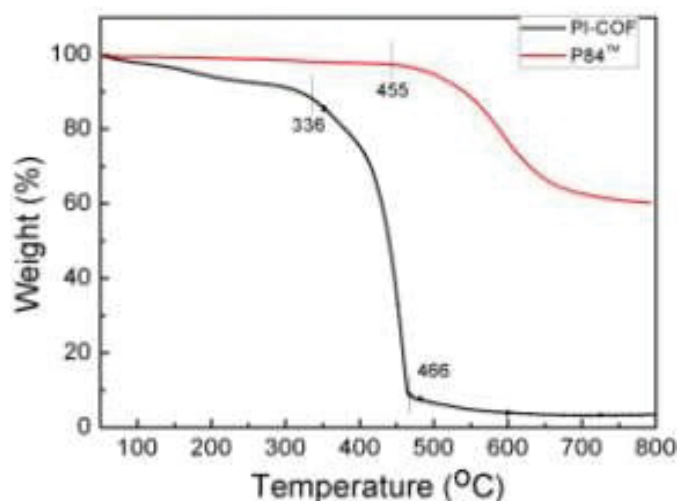


Figure 3: TGA curves of P84 (red) and PI-COF (black) under a nitrogen atmosphere and heating rate of 10°C/min.

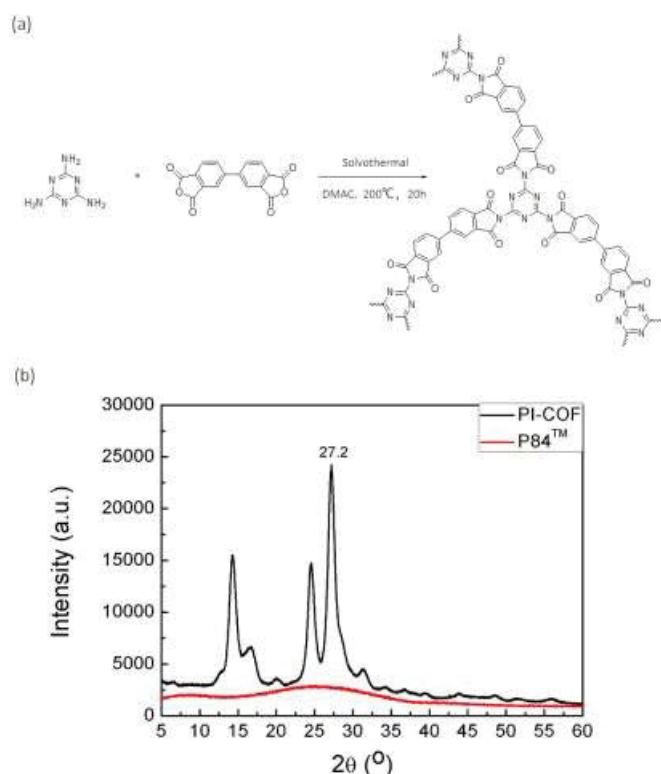


Figure 1: (a) Schematic pathway for PI-COF synthesis; (b) Powder XRD patterns of PI-COF and P84.

stretching vibrations, respectively. These results indicate polyimide framework of PI-COF is formed under our conditions.

Thermal stability of PI-COF was confirmed by the thermo gravimetric analysis (TGA) under nitrogen (Figure 3). From PI-COF TGA curves (black), it undergoes one-step thermal degradation processes before 336°C, which was attributed to the evaporation of trace residue solvent and further dehydration for imidization. The weight of PI-COF shows a rapid mass loss after 336°C, which demonstrates the thermal decomposition of triazine ring. The polymer backbone was destroyed as triazine decomposed quickly from 336 to 466°C. The results confirmed that the PI-COF displays good thermal stability, which may be attributed to the incorporation of the structurally both triazine rings and imide rings [32,33].

The porosity of PI-COF was measured by nitrogen sorption at 77 K. Figure 4a shows a sharp rise at high relative pressure ( $P/P_0=1$ ), suggesting the meso- or macropores involved in the PI-COF. Figure 4b shows the pore size distribution that is calculated from nonlinear density functional theory (NLDFT), which shows one peak at 36.2 Å. As agreeing with the nitrogen adsorption-desorption analytical curve, this pore size distribution curve confirmed that

the uniform meso-pores present in the PI-COF. The contribution of microporosity is only 0.77%, which is calculated by the ratio of t-Plot micropore volume ( $0.001019 \text{ cm}^3/\text{g}$ ) over the total pore volume ( $0.132292 \text{ cm}^3/\text{g}$ ). The BET surface area of this PI-COF is  $103.50 \text{ m}^2/\text{g}$  due to a higher conformational flexibility of the network by the biphenyl linker between the cross-linking melamine units [34].

### Characterization and performance of PI-COF doped membrane

Figure 5 show the SEM images of PI-COF doped MMM. As shown in Figure 5a, when doping PI-COF in the membrane, many bulges appeared on the surface, which implied some PI-COF particles agglomerated in the P84 matrix. With the increase of PI-COF loading, the aggregation becomes more significant (Figure 5a-5h). The images of the MMMs cross section shows that P84 tightly surrounds the PI-COF particles without voids at PI-COF loading of 10-30 wt%. Due to the existence of unreacted  $\text{NH}_2$  and  $\text{COOH}$  groups in the PI-COF, hydrogen bonds might be formed between the PI-COF and P84, making the PI-COF having a good affinity with P84 matrix. These closely embedded PI-COF could effectively improve the gas permeability and selectivity. The cross-section morphology showed the thickness of membrane is approximately 7-12  $\mu\text{m}$  with the PI-COF loading. From the SEM image of (Figure 5i), PI-COF particles were 1-2  $\mu\text{m}$  and the fluffy surface could be observed. The fluffy surface comes from inner porous structure destruction during milling.

To evaluate the separation performance of the PI-COF doped membrane, pure gas  $\text{O}_2$  and  $\text{N}_2$  were used respectively to test the permeability of MMMs at 0.1 MPa. As shown in Table 1, the oxygen and nitrogen permeability were obtained with 83 and 49 barrer, respectively, when 10 wt% PI-COF was doped in the membrane. Notably, the nitrogen permeation through MMM was higher than the oxygen with  $\text{N}_2/\text{O}_2$  ideal selectivity of 1.69. When the loading of PI-COF reached 20 wt%, the nitrogen permeability increased to 466 barrer with the highest selectivity of 2.13. The selectivity

**Table 1:** Gas permeability and selectivity of PI-COF doped MMM at 0.1 MPa.

PI-COF loading (wt%)	Permeability (barrer)		Ideal selectivity a, $\text{N}_2/\text{O}_2$
	$\text{N}_2$	$\text{O}_2$	
0	-	-	-
10	83	49	1.69
20	466	219	2.13
30	519	330	1.57
40	1915	1513	1.27

of  $\text{N}_2/\text{O}_2$  reduced to 1.57 at PI-COF 30 wt% loading. At 40 wt% loading of PI-COF, both nitrogen and oxygen had a sharply increasing permeability with 1915 and 1513 barrer, respectively, but  $\text{N}_2/\text{O}_2$  selectivity decreased to 1.27. For comparison, pristine P84 membrane without loading PI-COF gave no permeation of  $\text{O}_2$  and  $\text{N}_2$  at the same conditions.

It is considered that gas transport occurring in the dense polymeric membranes can be described by the solution diffusion mechanism [35,36]. The pristine P84 membrane impedes transport of  $\text{O}_2$  and  $\text{N}_2$  in our conditions, which suggests that solution diffusion is limited by the structure of P84. The PI-COF doped membranes showed good nitrogen permeability and  $\text{N}_2/\text{O}_2$  selectivity. This proves that the PI-COF particles acted as gas channels for gas permeation. The 36.2 Å mesoporosity presenting in the PI-COF is enough for  $\text{N}_2$  and  $\text{O}_2$  effective permeation. Gas transport through inorganic membranes including ceramic and carbon membranes is more complex than that of polymeric membranes. Basically, four mechanisms are considered as the Knudsen diffusion, the molecular sieving, the surface diffusion and the capillary condensation. In our case, the gas diffusion did not follow the order of gas molecular kinetic diameters ( $\text{O}_2=3.46 \text{ \AA}$ ,  $\text{N}_2=3.64 \text{ \AA}$ ), which suggested that molecular sieving mechanism can be ignored. The diffusion of  $\text{N}_2$  is faster than that of  $\text{O}_2$  through the PI-COF doped membrane, and the  $\text{N}_2/\text{O}_2$  permselectivity was 2.13, which was much higher than the Knudsen diffusion ratio ( $\text{N}_2/\text{O}_2=1.07$ ) [30]. Therefore, besides Knudsen diffusion, gas permeation was also controlled by surface diffusion mechanism due to permanent mesopores existing in the PI-COF. The surface diffusion increases the performance of gas transport via adsorption of gas on the inner pore surface of the COF.

Loading PI-COF ranged from 10 to 40 wt%, the permeability of nitrogen increases from 83 barrer to 1915 barrer and the permeability of oxygen increases from 49 barrer to 1513 barrer. The ideal  $\text{N}_2/\text{O}_2$  selectivity has the maximum value of 2.13, when the PI-COF loading reached 20 wt%. As more PI-COF particles doped in the MMM, the gas permeability was sharply increased and  $\text{N}_2/\text{O}_2$  selectivity decreased. The overabundance of PI-COF particles in MMM gave rise to serious aggregation of the particles and poor dispersion in matrix. The formation of voids in the interface between the aggregated COF particles was observed in FESEM. In addition, voids in the interface between P84 and PI-COF particles would be formed as well. The existence of these voids results in high permeability and sharply decreasing selectivity.

Therefore, the doped PI-COF property and the loading amount

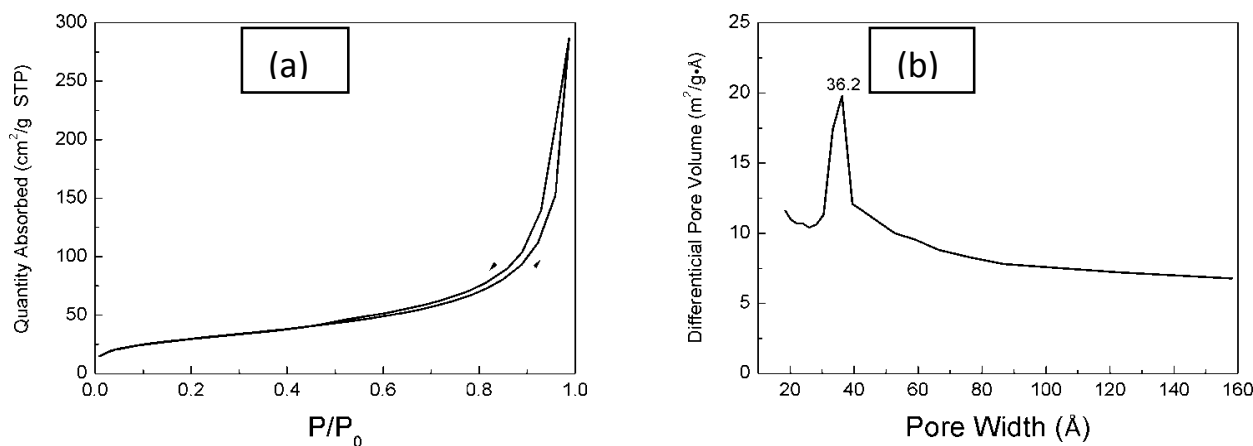


**Figure 4:** (a)  $\text{N}_2$  adsorption-desorption isotherms measured at 77 K; (b) Pore size distribution curves for PI-COF.

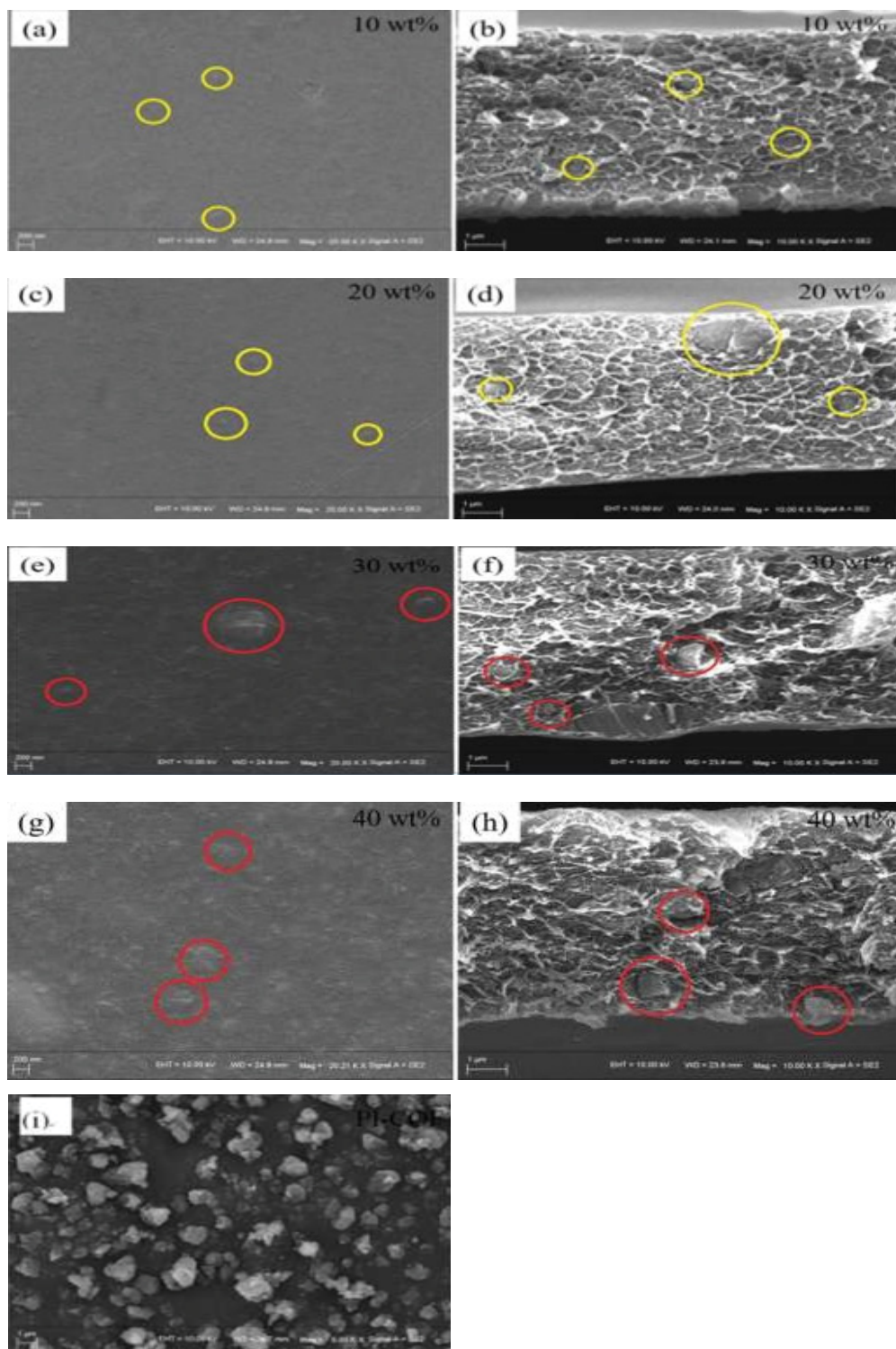


**Figure 5:** SEM images of MMMs with PI-COF particles of weight ratio from 10 to 40 wt% (a-h) and COF. Membrane surface (a, c, d, g) and cross section (b, d, f, h).

play an important role in the preparation of MMM. These results suggest that developing novel fillers with better compatibility between both polymer matrix and permeating gas is a key point to prepare a MMM with an excellent separation performance.

## CONCLUSION

The PI-COF had been synthesized by heating melamine and BPDA at 200°C in a solvothermal reactor. The crystalline and porous nanostructure of the PI-COF was confirmed via powder X-ray diffraction, FESEM and BET analysis. The meso-pores presenting in the PI-COF particles afforded enough channels for  $N_2$  and  $O_2$  permeation. As filler in MMM, the PI-COF doped P84

provided  $N_2$  permeability of 466 barrer and  $N_2/O_2$  ideal selectivity of 2.13. Nitrogen gas permeated faster through the MMM than  $O_2$ , which was associated with the surface diffusion mechanism. The oxygen molecules were intercepted on the feeding side of the membrane could be directly pumped into the combustion cell to enhance the burning. The results showed a possible way to developing new filler with simple synthesis and low cost to improve the MMM separation for oxygen enrichment.

## ACKNOWLEDGEMENT

We gratefully acknowledge financial support from the National Natural Science Foundation of China (21671148, 51602217). [1]

## REFERENCES

- Blume I, Pinnau I. Composite membrane, method of preparation and use. Patent No. 4,963,165. Washington, D.C.: U.S. Patent and Trademark Office. 1990.
- Kimura SG, Browall WR. Membrane oxygen enrichment: I. Demonstration of membrane oxygen enrichment for natural gas combustion. *J Membrane Sci.* 1986;29:69-77.
- Dean AM, Bozzelli JW. Combustion chemistry of nitrogen. In W.C. Gardiner (Ed.) *Gas-Phase Combustion Chemistry*, Springer New York, NY. 2000;125-341.
- Poola RB, Sekar R. Reduction of NO<sub>x</sub> and particulate emissions by using oxygen-enriched combustion air in a locomotive diesel engine. *J Eng Gas Turbines Power.* 2003;125:524-533.
- Lin H. Novel membranes and processes for oxygen enrichment. Office of scientific and technical information report, United States. 2011;1-33.
- <https://patents.google.com/patent/US20100176364>
- Lai JY, Wu GJ, Shyu SS. TPX/siloxane blend membrane for oxygen enrichment. *J Appl Polym Sci.* 1987;34:559-569.
- Baker RW. Future directions of membrane gas separation technology. *Ind Eng Chem Res.* 2002;41:1393-1411.
- Robeson LM. The upper bound revisited. *J Membrane Sci.* 2008;320:390-400.
- Chen JT, Shih CC, Fu YJ, Huang SH, Hu CC, Lee KR, et al. Zeolite-filled porous mixed matrix membranes for air separation. *Ind Eng Chem Res.* 2014;53:2781-2789.
- Goh PS, Ng BC, Ismail AF, Sanip SM, Aziz M, Kassim MA. Effect of dispersed multi-walled carbon nanotubes on mixed matrix membrane for O<sub>2</sub>/N<sub>2</sub> separation. *Sep Sci Technol.* 2011;46:1250-1261.
- Ismail AF, Rahman WR, Aziz F. Development of polysulfone (PSF)-carbon molecular sieve (CMS) mixed matrix membrane (MMM) for O<sub>2</sub>/N<sub>2</sub> gas separation. *AIP Conference Proceedings.* 2009;1136:201-206.
- Hashemifard SA, Ismail AF, Matsuura T. Mixed matrix membrane incorporated with large pore size halloysite nanotubes (HNTs) as filler for gas separation: morphological diagram. *Chem Eng J.* 2011;172:581-590.
- Kang Z, Peng Y, Qian Y, Yuan D, Addicoat MA, Heine T, et al. Mixed matrix membranes (MMMs) comprising exfoliated 2D covalent organic frameworks (COFs) for efficient CO<sub>2</sub> separation. *Chem Mater.* 2016;28:1277-1285.
- Shan M, Seoane B, Andres-Garcia E, Kapteijn F, Gascon J. Mixed-matrix membranes containing an azine-linked covalent organic framework: Influence of the polymeric matrix on post-combustion CO<sub>2</sub> capture. *J Membrane Sci.* 2018;549:377-384.
- Wu X, Tian Z, Wang S, Peng D, Yang L, Wu Y, et al. Mixed matrix membranes comprising polymers of intrinsic microporosity and covalent organic framework for gas separation. *J Membrane Sci.* 2017;528:273-283.
- Duan K, Wang J, Zhang YT, Liu JD. Covalent organic frameworks (COFs) functionalized mixed matrix membrane for effective CO<sub>2</sub>/N<sub>2</sub> separation. *J Membrane Sci.* 2019;572:588-595.
- Katekomol P, Roeser J, Bojdys M, Weber J, Thomas A. Covalent triazine frameworks prepared from 1,3,5-Tricyanobenzene. *Chem Mater.* 2013;25:1542-1548.
- Biswal BP, Chaudhari HD, Banerjee R, Kharul UK. Chemically 14 stable covalent organic framework (COF)-Polybenzimidazole hybrid membranes: Enhanced gas separation through pore modulation. *Chem Eur J.* 2016;22:4695-4699.
- Ismail AF, Khulbe KC, Matsuura T. *Gas separation membranes: Polymeric and inorganic.* Springer. 2015;7.
- Fang Q, Wang J, Gu S, Kaspar RB, Zhuang Z, Zheng J, et al. 3D Porous crystalline polyimide covalent organic frameworks for drug delivery. *JACS.* 2015;137:8352-8355.
- Zornoza B, Esekhiile O, Koros WJ, Tellez C, Coronas J. Hollow silicalite-1 sphere-polymer mixed matrix membranes for gas separation. *Sep Purif Technol.* 2011;77:137-145.
- Widjojo N, Chung TS, Kulprathipanja S. The fabrication of hollow fiber membranes with double-layer mixed-matrix materials for gas separation. *J Membrane Sci.* 2008;325:326-335.
- Bae TH, Liu J, Lee JS, Koros WJ, Jone CW, Nair S. Facile high-yield solvothermal deposition of inorganic nanostructures on zeolite crystals for mixed matrix membrane fabrication. *JACS.* 2009;131:14662-14663.
- Clarizia G, Algieri C, Regina A, Drioli E. Zeolite-based composite PEEK-WC membranes: gas transport and surface properties. *Micropor Mesopor Mat.* 2008;115:67-74.
- Bastani D, Esmaili DN, Asadollahi M. Polymeric mixed matrix membranes containing zeolites as a filler for gas separation applications: A review. *J Ind Eng Chem.* 2013;19:375-393.
- Maier G, Wolf M, Bleha M, Pientka Z. Gas permeabilities of polymers with indan groups in the main chain.: 2: Polyimides. *J Membrane Sci.* 1988;143:115-123.
- Shen Y, Lua AC. Structural and transport properties of BTDA-TDI/MDI co-polyimide (P84)-silica nanocomposite membranes for gas separation. *Chem Eng J.* 2012;188:199-209.
- Xu L, Zhang C, Rungta M, Qiu W, Liu J, Koros WJ. Formation of defect-free 6FDA-DAM asymmetric hollow fiber membranes for gas separations. *J Membrane Sci.* 2014;459:223-232.
- Illing G, Hellgardt K, Wakeman RJ, Jungbauer A. Preparation and characterization of polyaniline based membranes for gas separation. *J Membrane Sci.* 2001;184:69-78.
- Zhao H, Xie Q, Ding X, Chen J, Hua M, Tan X. High performance post-modified polymers of intrinsic microporosity (PIM-1) membranes based on multivalent metal ions for gas separation. *J Membrane Sci.* 2016;514:305-312.
- Wang X, Hu Y, Song L, Xing W, Lu H, Lv P, et al. Effect of a triazine ring-containing charring agent on fire retardancy and thermal degradation of intumescent flame retardant epoxy resins. *Polym Advan Technol.* 2011;22:2480-2487.
- Kim IC, Kim JH, Lee KH, Tak TM. Phospholipids separation (degumming) from crude vegetable oil polyimide ultrafiltration membrane. *J Membrane Sci.* 2002;205:113-123.
- Schwab MG, Fassbender B, Spiess HW, Thomas A, Feng X. Catalyst-free preparation of melamine-based microporous polymer networks through schiff base chemistry. *J Am Chem Soc.* 2009;131:7216-7217.
- Wijmans JG, Baker RW. The solution-diffusion model: A review. *J Membrane Sci.* 1995;107:1-21.
- Paul DR. Reformulation of the solution-diffusion theory of reverse osmosis. *J Membrane Sci.* 2004;241:371-386.